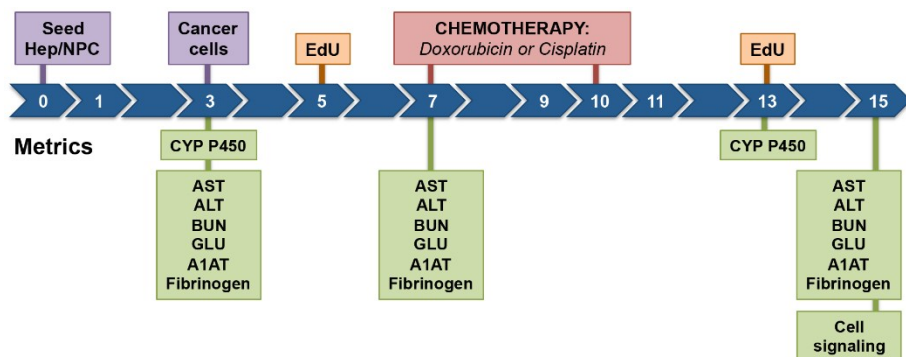
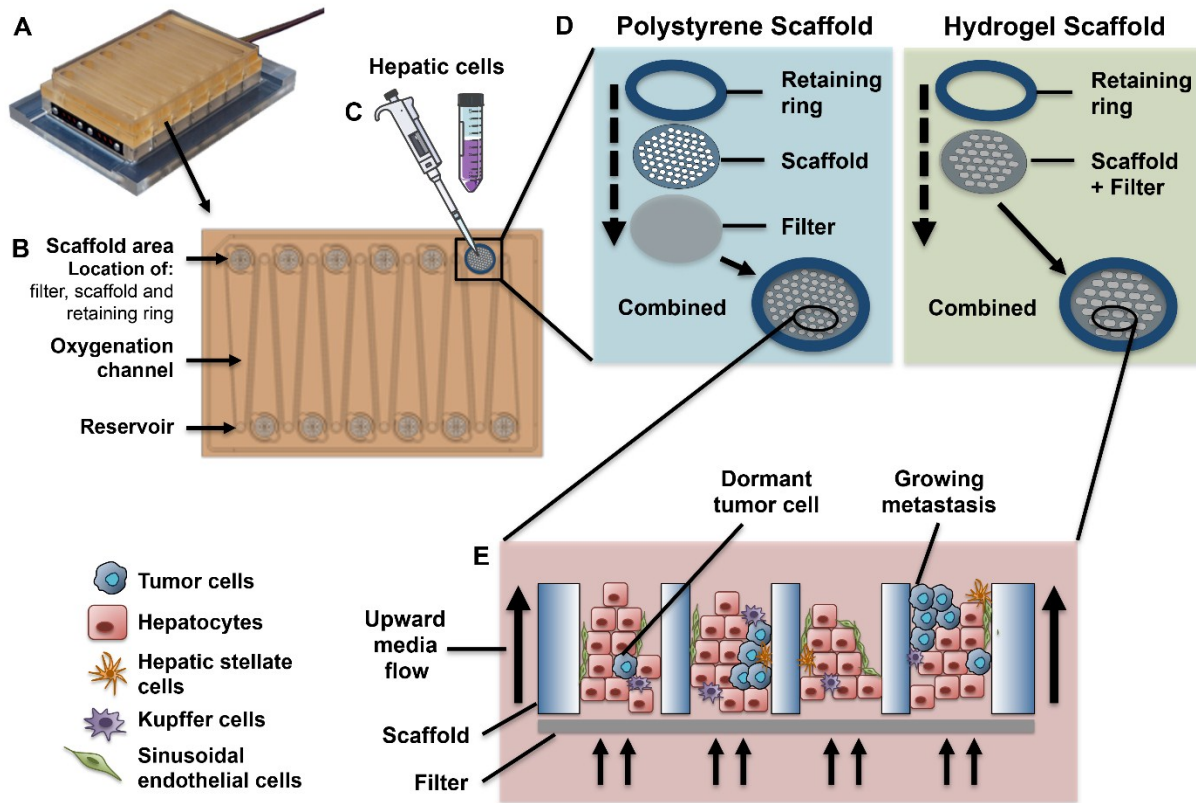


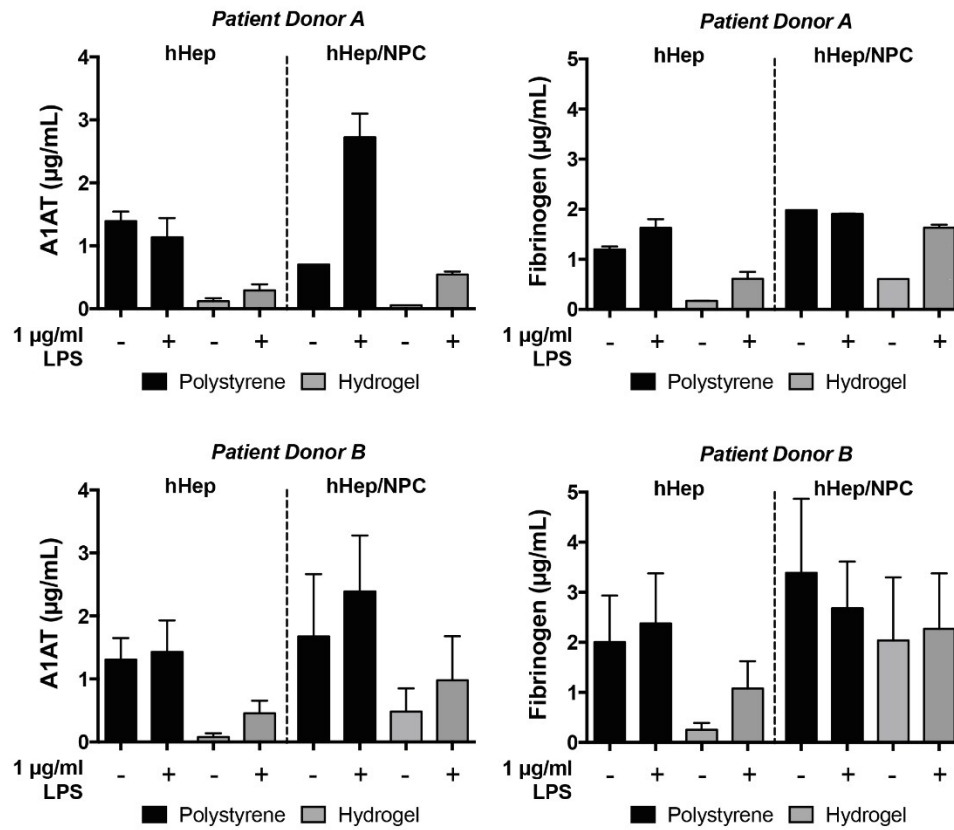
SUPPLEMENTARY FIGURE LEGENDS



Supplemental Figure 1: Experimental overview. A daily timeline of additions to the scaffolds (above the timeline) and assessments (below the timeline).

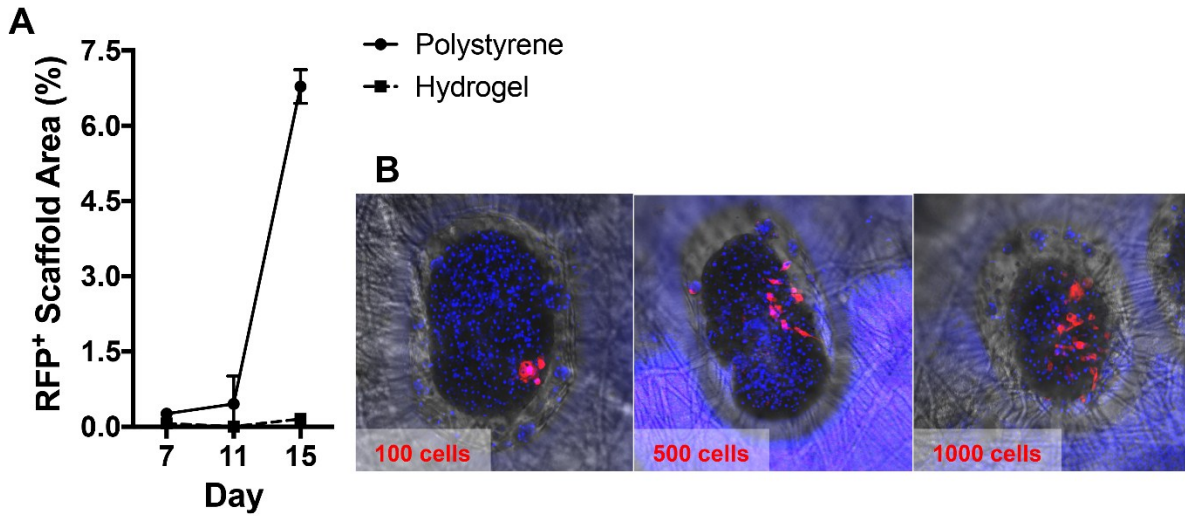


Supplemental Figure 2: Construction and seeding schematic for the metastatic LiverChip microphysiological system (adapted from Clark *et. al.* ¹⁴). (A) The fully constructed LiverChip depicted within its docking station. (B) Aerial view of the top plate showing the 12 individual liver-units, the location where hepatic cells are seeded and micro-tissue forms. (C) Cells are directly seeded onto an imprinted scaffolding unit, which (D) comprises a layering of a scaffold on top of a 0.22 μm PVDF filter, secured in place by a retaining ring. Note: for the hydrogel scaffolds, the PVDF filter is pre-attached. (E) The actual micro-tissue resides in multiple channels that approach the size of a liver lobule. Within these tissues, tumor cells may intravasate and a subset outgrow immediately, while another spontaneously undergo dormancy. Fluid flow up through the microtissue supports hepatic tissue development and provides a constant supply of re-oxygenated medium enabling prolonged culture).



Supplemental Figure 3: Acute phase proteins production following stimulation with LPS.

Levels of acute phase proteins, A1AT and fibrinogen, were measured by ELISA on day 15 following stimulation with 1 µg/mL LPS for 24 hours (n = 2 donors in duplicate). Graphs depict absolute concentration (µg/mL) proteins produced by each patient donor. Significant differences were determined via non-parametric pairwise Wilcoxon rank sum tests (*p<0.05).



Supplemental Figure 4: Hydrogel scaffolds provide a more physiological microenvironment that allows for improved recapitulation of dormancy. On day 3, hepatic tissue supported by hydrogel scaffolds was seeded with MDA-MB-231 cells expressing RFP. (A) Wells were seeded with 500 cells and complete scaffolds were imaged in the RFP channel (2x objective) and the percent of total area positive for RFP was calculated on day 7, 11, and 15 (n = 1 donors). (B) A relatively minor increase in breast cancer cells present in the metastatic niche after 12 days from 100 to 1000 cells/wells indicated the proliferative capacity to be either reduced or completely halted.

SUPPLEMENTAL MATERIALS

Supplemental Table S1. Assay performance characteristics and curve fit statistics using 5 parameter logistic (5 PL) regression of standards

Analytes	Alternate Names	Bead Region	Dilution Factors	Assay Working Range		Assay Sensitivity	5 PL Curve Fit Statistics			
				LLoQ	ULoQ	LoD	Residual Variance	Fit Probability	Degrees of Freedom	wSSE
				(pg/mL)		(pg/mL)				
<i>Human group I, 27-plex panel</i>										
IL-1 β		39	1.0	0.5	518	0.3	0.55	0.74	5	2.75
IL-1Ra		25	1.0	5.0	4,557	4.5	0.14	0.98	5	0.68
IL-2		38	1.0	0.9	1,041	1.2	0.48	0.79	5	2.41
IL-4		52	1.0	0.3	279	0.1*	0.63	0.64	4	2.52
IL-5		33	1.0	1.5	1,441	1.9	0.70	0.59	4	2.80
IL-6		19	1.0, 0.06	2.4	2,168	1.2	0.78	0.54	4	3.13
IL-7		74	1.0	0.8	996	0.5	1.20	0.31	4	4.82
IL-8		54	1.0, 0.06	2.8	2,442	0.7	0.82	0.53	5	4.12
IL-9		77	1.0	1.2	1,537	1.5	0.61	0.65	4	2.45
IL-10		56	1.0	2.2	2,232	1.4	0.57	0.68	4	2.29
IL-12p70		75	1.0	2.6	2,585	2.4	0.23	0.95	5	1.16
IL-13		51	1.0	0.5	482	0.4	0.60	0.73	6	3.62
IL-15		73	1.0	1.5	293	1.7	0.35	0.91	6	2.12
IL-17A		76	1.0	4.0	1,838	4.0	1.01	0.41	5	5.04
Eotaxin		43	1.0	7.0	1,667	3.5	1.61	0.19	3	4.82
Basic FGF		44	1.0	8.2	1,038	3.8	0.63	0.70	6	3.79
G-CSF		57	1.0	2.5	2,328	0.9	0.65	0.63	4	2.60
GM-CSF		34	1.0	2.9	753	3.0	0.45	0.84	6	2.71
IFN- γ		21	1.0	4.0	1,899	5.5	1.08	0.37	6	6.48
IP-10		48	1.0, 0.25, 0.125	9.0	2,185	7.1	1.85	0.12	4	7.38
MCP-1	MCAF	53	1.0	1.5	1,532	3.1	0.40	0.88	6	2.43
MIP-1 α		55	1.0	0.0	61	0.1	0.40	0.88	6	2.39
MIP-1 β		18	1.0	1.3	577	0.7	0.30	0.93	6	1.83
PDGF-BB		47	1.0	19.6	1,602	2.4	1.85	0.12	5	7.38
RANTES		37	1.0	0.7	1,041	2.4	0.45	0.84	6	2.73
TNF- α		36	1.0	4.0	3,945	2.7	1.33	0.25	5	6.64
VEGF-A		45	1.0	1.8	1,950	2.6	0.21	0.93	4	0.84
<i>Chemokines, 40-plex panel</i>										
6Ckine	CCL21	12	1.0	101.4	9,849	53.7	1.81	0.08	7	12.65

BCA-1	CXCL13	74	1.0	0.5	1,438	0.5	1.22	0.29	7	8.56
CTACK	CCL27	72	1.0	8.7	4,754	4.0	1.08	0.37	7	7.58
Eotaxin	CCL11	43	1.0	8.3	542	7.7	4.03	0.00	5	20.13
Eotaxin-2	CCL24	30	1.0	9.1	1,555	28.0	0.94	0.45	5	4.71
Eotaxin-3	CCL26	65	1.0	11.2	1,031	8.1	0.79	0.56	5	3.95
Fractalkine	CX3CL1	77	1.0	14.1	11,432	5.0	1.79	0.10	6	10.76
GCP-2	CXCL6	15	1.0	6.1	2,409	11.4	1.23	0.28	7	8.61
GM-CSF		34	1.0	18.2	2,113	9.9	1.78	0.31	6	10.67
Gro- α	CXCL1	61	1.0, 0.25	30.1	1,772	20.5	1.32	0.25	5	6.60
Gro- β	CXCL2	78	1.0, 0.25	12.4	4,659	23.2	1.02	0.41	7	7.17
I-309	CCL1	20	1.0	40.7	2,289	16.3	2.09	0.05	6	12.55
IFN- γ		21	1.0	8.8	927	5.1	1.92	0.12	3	5.77
IL-1 β		39	1.0	4.8	585	0.1*	2.41	0.03	6	14.44
IL-2		38	1.0	5.6	3,445	3.8	0.86	0.53	7	6.04
IL-4		52	1.0	19.6	608	19.7	0.77	0.51	3	2.31
IL-6		19	1.0	0.9	2,246	0.9	0.89	0.51	7	6.25
IL-8	CXCL8	54	1.0	0.6	525	0.4	0.91	0.49	6	5.46
IL-10		56	1.0	6.0	3,826	2.3	1.88	0.08	6	11.29
IL-16		27	1.0	16.7	8,824	9.6	1.05	0.39	7	7.37
IP-10	CXCL10	48	1.0	5.8	5,040	3.6	1.21	0.30	6	7.25
I-TAC	CXCL11	25	1.0	1.1	227	0.3	1.03	0.41	7	7.22
MCP-1	CCL2	53	1.0	0.3	256	0.0	0.99	0.43	6	5.95
MCP-2	CCL8	57	1.0	0.3	1,162	0.2	1.38	0.21	7	9.65
MCP-3	CCL7	26	1.0	16.8	2,345	20.1	1.26	0.27	7	8.79
MCP-4	CCL13	28	1.0	1.4	214	2.8	0.84	0.54	6	5.01
MDC	CCL22	29	1.0	10.0	740	9.3	4.26	0.00	4	17.02
MIF		35	1.0, 0.25	143.6	97,939	54.0	0.88	0.51	6	5.30
MIG	CXCL9	14	1.0	12.6	1,567	5.4	0.11	1.73	6	0.65
MIP-1 α	CCL3	55	1.0	3.1	371	0.5	2.99	0.01	6	17.94
MIP-1 δ	CCL15	66	1.0, 0.5, 0.25	35.0	1,223	8.4	1.74	0.11	6	10.45
MIP-3 α	CCL20	62	1.0	3.9	1,739	0.9	0.52	0.82	7	3.63
MIP-3 β	CCL19	76	1.0	29.9	3,054	11.0	3.32	0.01	4	13.28
MPIF-1	CCL23	37	1.0	8.7	5,097	3.2	0.92	0.49	7	6.46
SCYB16	CXCL16	64	1.0	14.0	1,607	3.6	1.39	0.20	7	9.76
SDF-1 α + β	CXCL12	22	1.0	42.8	2,342	28.6	1.03	0.40	7	7.24
TARC	CCL17	67	1.0	10.3	4,638	11.5	3.17	0.01	5	15.83
TECK	CCL25	46	1.0	70.9	32,589	14.1	1.00	0.43	7	6.97
TNF- α		36	1.0	6.3	3,114	1.1	0.89	0.51	7	6.26
<i>Human Cancer Panel 1, 16-plex</i>										
sEGFR	ErbB1,	15	1.0	6.2	7,475	7.9	0.99	0.41	9	3.94

	EGFR1									
FGF-basic	FGF2, BFGF	44	1.0	0.7	1,690	0.8	0.94	0.44	9	3.75
Follistatin	FSN	26	1.0	257.5	8,815	611.9	0.69	0.66	11	4.13
G-CSF		57	1.0	0.6	4,235	0.8	0.20	0.98	11	1.18
HGF	SF	62	1.0	17.3	9,391	2.4	0.22	0.95	10	1.10
sHER-2/neu	ErbB2	12	1.0	21.3	9,257	0.0	0.70	0.63	10	3.48
sIL-6R α	CD126	19	1.0	2.0	3,842	0.7	0.24	0.96	11	1.45
Leptin		78	1.0	3.8	3,523	4.6	0.93	0.47	11	5.56
Osteopontin	OPN	77	0.25	12.8	18,611	18.8	0.19	0.98	11	1.16
PDGF-AB/BB		47	1.0	15.2	8,809	6.4	0.58	0.75	11	3.45
PECAM-1	CD31	46	1.0	39.3	4,911	19.0	0.70	0.65	11	4.20
Prolactin	PRL	52	1.0	92.7	33,160	33.0	0.27	0.95	11	1.63
SCF	KL1	65	1.0	1.3	2,682	6.8	0.27	0.95	11	1.64
sTIE-2	CD202b	64	1.0	8.2	65,521	14.0	0.17	0.98	11	1.02
sVEGFR-1	FLT1	76	1.0	246.1	9,174	96.5	0.36	0.91	11	2.14
sVEGFR-2	KDR, FLK1	45	1.0	6.4	64,137	9.4	0.68	0.64	10	3.42
<i>Human Cancer Panel 2, 18-plex</i>										
Angiopoietin-2		47	1.0	43.0	23,300	89.4	2.35	0.04	10	11.76
sCD40L	TRAP	29	1.0	3.0	12,629	2.9	0.58	0.68	9	2.32
EGF		14	1.0	4.3	1,916	6.2	0.62	0.74	12	4.31
Endoglin	CD105	26	1.0	6.0	35,998	2.7	0.97	0.44	10	4.83
sFASL	CD95L, APO-1L	35	1.0	104.1	17,607	82.3	0.97	0.45	12	6.82
HB-EGF		57	1.0	5.2	1,761	1.3	1.10	0.36	12	7.70
IGFBP-1		62	1.0, 0.25	3.9	18,984	18.7	0.41	0.90	12	2.85
IL-6		19	1.0	0.9	5,344	0.2	2.13	0.05	11	12.78
IL-8	CXCL8	54	1.0	0.4	2,212	0.1*	0.64	0.72	12	4.48
IL-18		42	1.0	1.5	10,529	0.1*	1.38	0.22	11	8.30
PAI-1	SERPINE1	61	0.25, 0.125, 0.03, 0.01	16.2	34,428	9.0	1.96	0.07	11	11.77
PLGF	PGF	52	1.0	3.9	6,796	0.1*	1.29	0.26	10	6.47
TGF- α		76	1.0	2.0	3,545	0.1*	0.91	0.50	12	6.38
TNF- α		36	1.0	3.3	4,967	0.1*	2.93	0.01	11	17.56
uPA	Urokinase	78	1.0	1.0	7,576	0.1*	1.21	0.29	12	8.46
VEGF-A	VPF	45	1.0	52.5	16,537	84.2	0.43	0.88	12	3.03
VEGF-C	Flt4 ligand	64	1.0	17.8	26,230	15.2	0.97	0.45	13	7.79
VEGF-D	FIGF	43	1.0	97.7	44,382	126.2	0.76	0.62	12	5.35

LLoQ and ULoQ are the lower and upper limits of quantification where measurements are both accurate and precise. LoD, the limit of detection, is determined by adding two standard deviations to background MFI (Median Fluorescence Intensity) then extrapolating its concentration from the standard curve. Curve fit statistics of standards were calculated using the 5 parameter logistic regression model. Curve fits adjust parameters to minimize weighted sum of squared errors, i.e., wSSE. Initial assessments of curve-fitting include the residual variance, as defined by wSSE divided by the number of degrees of freedom accounted for within the immunoassay. The number of degrees of freedom is calculated as the number of data points in the standard curve minus the number of parameters in the curve model, i.e., 5 PL regression model equates to five parameters. As the wSSE has been shown to obey a chi-square distribution with the number of degrees present in an assay, fit probability is a metric that evaluates the curve fit; 1 is indicative of a perfect fit and 0 denotes a lack thereof.